PROCEEDINGS OF SCIENCE

The Cosmic Ray Event Spectrum in the Knee Region measured by the NICHE Array at Telescope Array

Douglas Bergman[a,*] **and Isaac Buckland**[a] **on behalf of the Telescope Array collaboration**

[a] *Dept. of Physics & Astronomy and High Energy Astrophysics Inst., University of Utah, Utah, USA*

E-mail: bergman@physics.utah.edu

The NICHE array at Telescope Array is a non-imaging Cherenkov light detector situated close to the Telescope Array Middle Drum fluorescence detector site. It has been operating since September 2017. Data collected between June 2020 and July 2024 has been analyzed and we will present the energy spectrum of the cosmic rays observed. The threshold energy of the detector is about 1 PeV and the data collected gives significant statistics up to about 100 PeV. The energy reconstruction used in this analysis uses the CHASM model, a model which incorporates extensive air shower universality and Cherenkov photon production.

39th International Cosmic Ray Conference (ICRC2025)
15–24 July 2025
Geneva, Switzerland

ICRC 2025
The Astroparticle Physics Conference
Geneva July 15-24, 2025

*Speaker

PoS(ICRC2025)188

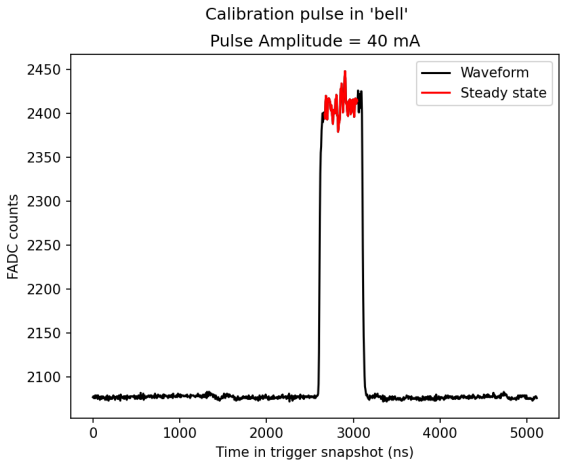

Figure 1: Example response of counter *bell* to a 40-mA pulse

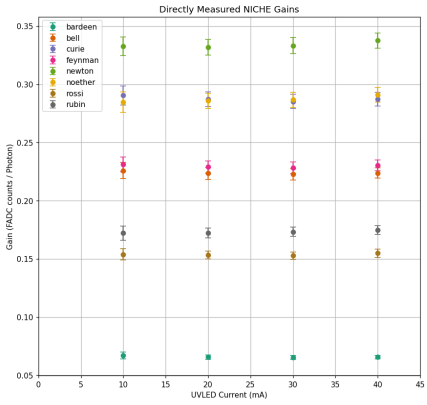

Figure 2: Measured, absolute NICHE counter gains vs. the four UVLED pulse currents.

This measurement of the cosmic ray energy spectrum uses the Non-Imaging CHErenkov Array (NICHE) which is a low energy extension of the Telescope Array (TA) observatory. This measurement is a follow-up to the spectrum measurement presented at the 2021 ICRC [1], but using data different period, an in-site end-to-end calibration, and making use of the CHASM [2] model both in the reconstruction of air-shower parameters and in the simulation of the detector aperture. The data used was collected between June 2021 and July 2024, but with some of 2021 and all of 2022 absent due to a data loss issue.

An *in situ* calibration was performed on 14 April 2024. A UV LED light source was used to illuminate each of eight working counters. The UV LED light source is used for gain matching the photomultiplier tubes of the TA fluorescence detector mirrors. The UV LED was itself calibrated against a test TA FD mirror in the lab, to determine its absolute light output at current settings 10, 20 30, and 40 mA. An example response to the calibration for the NICHE counter *bell* is shown in Figure 1. The result of the calibrations for all eight counters is shown in Figure 2. The calibration is an end-to-end photometric calibration and includes both quantum efficiency, collection efficiency and the transmission through the glass of the NICHE counter. The planned gain of the PMTs was to have about one FADC count per photoelectron, and most of the gains observed are consistent with that, the counter *bardeen* being the clear exception with a very low gain.

The absolute calibration from 14 April 2024 was projected backward and forward in time using the the open-shutter/closed-shutter noise files taken every hour for each counter during normal operation. Open-shutter noise is dominated by the night sky photon background, and assuming this background rate is contstant for clear observing condition allows one to estimate the gain from the RMS of the noise signal. Since the sampling rate is shorter than the time constant of the data acquisition system, we actually look at the average power of a fast fourier transform of the noise. This also allows us to remove the effect of an electronics-noise murmur evident in the FFT signals. We subtract the average power of the shutter-closed FFT from the average power of the shutter-open signal to isolate the effect of the night-sky background itself. The differenced-power on the low-frequency plateau is the variance of the FADC signal due to the night-sky background, away from

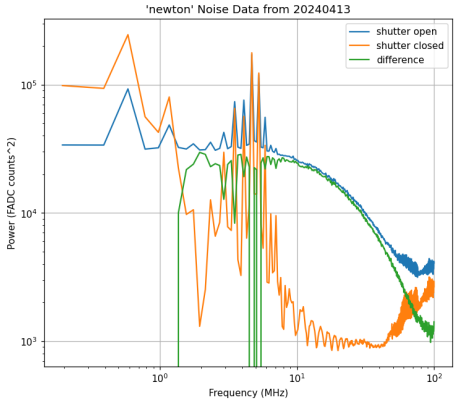

Figure 3: The average power from 4096 shutter-open noise waveforms, from 4096 shutter-closed waveforms, and their difference. The plateau in the difference at frequencies below 10 MHz, is the variance in the FADC values due to the night-sky background.

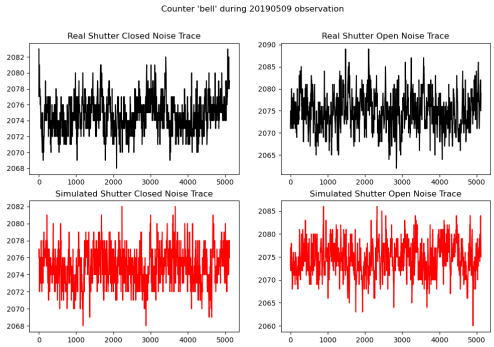

Figure 4: Simulated noise traces using the method described in the text. The upper row shows actual, collected noise traces, closed-shutter on the left, open-shutter on the right. The lower rows shows the simulated noise for each, respectively, using stored open and closed shutter data from the same data-part.

the bin-to-bin correlations of the data-acquisition system and with the electronics noise removed. If the night-sky background rate is constant, this is a measurement of the gain. We don't quote a measurement of the night-sky background rate itself due to uncertainties in angular acceptance and spectral response of the counters. An example of one shutter-open/shutter-closed measurement is shown in Figure 3.

The electronics noise evident in the FFT frequency response shown in Figure 3 must be simulated if one is to properly simulate the response of the detector array to cosmic rays. A sub-threshold signal may be pushed over the trigger threshold if it comes at the same time as an electronics noise pulse maximum. To characterize the electronics noise, the shutter-open and shutter-closed noise files are analyzed by FFT, forming both the amplitude and phase histograms at each frequency. To create a simulated noise waveform (upon which to eventually add simulated signal) one selects amplitude and phase from the histograms at random to form one frequency-domain noise sample and then applies the inverse-FFT to get a time-domain noise signal. This procedure works well, and does not reuire the characterization of the noise pulse. An example of simulating the noise is shown in Figure 4.

The response of the NICHE counters to cosmic ray air showers was performed using the CHASM simulation [2]. Rather than using a phenomenological fit to the counter signals, as was done in [1], an air shower with a given depth profile of shower particles, *i.e.* with a given energy, $X_{\max}$ and $N_{\max}$ is posited, the detector response is generated and a cost function is minimized against the shower parameters. In this analysis counter-level pulse features including pulse time, amplitude, rise time, fall time, and pulse area are simulated and compared to data in fitting the shower parameters. A simplex algorithm is used to do the fitting to find the shower parameters of core position, arrival direction, $N_{\max}$, and $X_{\max}$.

The CHASM simulation is also used to simulate the detector aperture. In this use of the model,

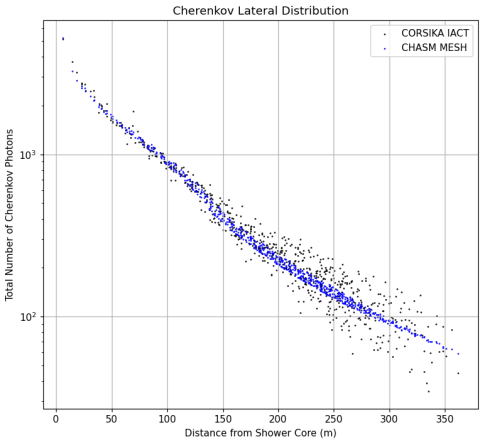

Figure 5: The lateral distribution of Cherenkov photons as generated by CHASM (blue) and as generated by CORISKA-IACT (black). This shower was simulated in CORSIKA as a proton with energy 1.14 PeV and a zenith angle of 20°. The CORSIKA longitudinal profile was recorded and used in the CHASM simulation.

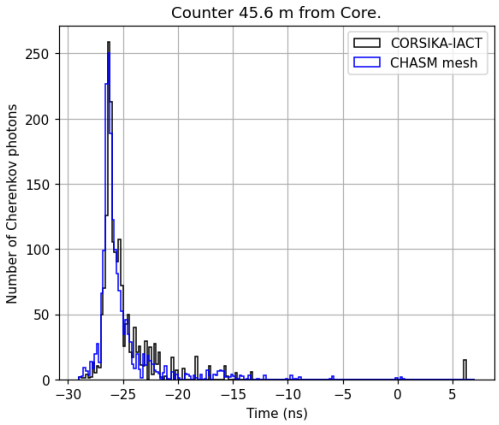

Figure 6: The arrival time distribution of photons on a counter using the same event as simulated in Figure 5. The time is with respect to the core would receive light. The zenith angle and the location of the counter underneath the shower give rise to the early photon times.

noise is also generated as described above. The CHASM simulation models the lateral as well as the longitudinal generation of Cherenkov light, but it does not simulate the effect of hadronic sub-showers in the data. This will have an effect on the aperture, when the average level of Cherenkov light in a shower would be insufficient to trigger a counter, but a counter would be triggered if a sub-shower were directed toward it. An example of the lateral response of counters to the CHASM model is compared to a CORSIKA-IACT [3] generated response in Figure 5. The greater variation in number of photons at a given distance from the shower core is due to hadronic sub-showers in CORSIKA.

CHASM simulates the time arrival of photons well. An example is shown in Figure 6. This allows the use of the width FADC pulses in fitting showers.

Events are reconstructed beginning with a characterization of the counter pulse widths. All the triggered FADC traces are fit to a functional form used by the Tunka Experiment [4]. This fit includes a peak amplitude, peak time, rise time, fall time and a baseline. An example fit is shown in Figure 7 using a waveform from the *newton* counter. This analysis will use the peak time and the integrated pulse area from these fits.

From the trigger time of the counters coincidences are formed for counters within 100 μs. We will require a 6-fold coincidence for events in this work (this is the same level as in [1]. A fit for the arrival direction is performed using the assumption of a plane Cherenkov wavefront and using the fit pulse times. A rough determination of the center of the event is performed by taking the integral pulse-weighted center-of-mass. (The pulse integral is adjusted according to the gain of the counter in this calculation).

With a rough determination of the shower parameters, a fit using the CHASM simulation is

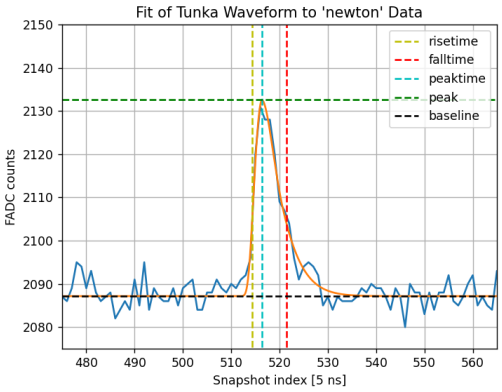

Figure 7: AN example fit the a recorded waveform from *newton*. The fit [4] gives a peak time, peak amplitude, rise time, fall time, and a baseline. The parameters also give an integrated pulse area over the baseline.

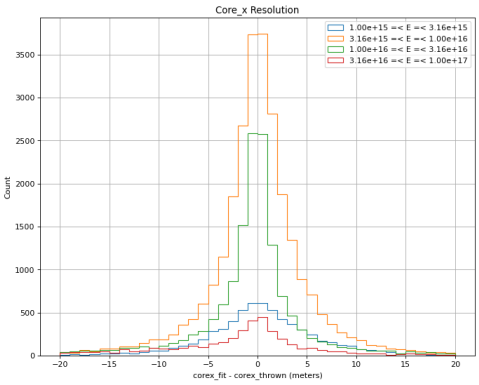

Figure 8: The core position resolution in the x (E-W) direction. The resolution is shown for half-decade in energy bands which are not normalized and thus represent the thrown E^{-2} spectrum combined with trigger efficiency.

performed in an inverse Monte Carlo fashion. The fit is done using the simplex method rather than the traditional gradient descent method due to details of CHASM simulation which give a non-smooth cost function. No FADC noise is simulated by CHASM in this use of the model. The fitting procedure is as follows. Using just the total signal, and the plane-fit estimate of the zenith angles, a guess at profile parameters is made using a compiled MC simulation. This gives only a very rough value of $X_{\max}$ (within $\sim$ 100 g/cm^2) and an order-of-magnitude estimate of $N_{\max}$. Then, with core position and shower longitudinal parameters fixed, the arrival direction is fit using the peak times of the counters. The final fitting, with the arrival directions updated and fixed, consists of allowing the core position and the two profile parameters to vary while minimizing using only the integrated pulse areas as features.

The results of fitting on CHASM-generated proton induced air-showers is as follows. The core position resolution is $\sim$ 2 m. An example of the resolution in the E-W direction is shown in Figure 8. The zenith angle resolution is of order of a tenth of a degree, while the azimuthal angle is of order a few tenths of a degree (all the zenith angles are $< 40^\circ$ so a the azimuthal angle should include a $\sin\theta$ factor for this comparison). The zenith angle resolution is shown in Figure 9. The measured energy of a shower is closely related to the determination of $N_{\max}$. In the range 3–30 PeV, $N_{\max}$ resolution is better than 10%. There is a loss of resolution and some bias at the highest energies due to the limited size of the NICHE array. $N_{\max}$ resolution in shown in Figure 10. The energy of the shower is determined from integrating the Gaisser-Hillas distribution determined from $N_{\max}$ and $X_{\max}$ measurements. An anti-correlation between the fit of $N_{\max}$ and $X_{\max}$ provides somewhat better energy resolution at the highest energies than the observed $N_{\max}$ resolution.

The aperture for this measurement was determined by MC simulation using a library of proton induced shower profiles generated by CORSIKA and then simulated using the CHASM program for the Cherenkov light production. The trigger for counters was simulated as described above using night-by-night gain data and detector statuses. These MC generated data were used in the resolution

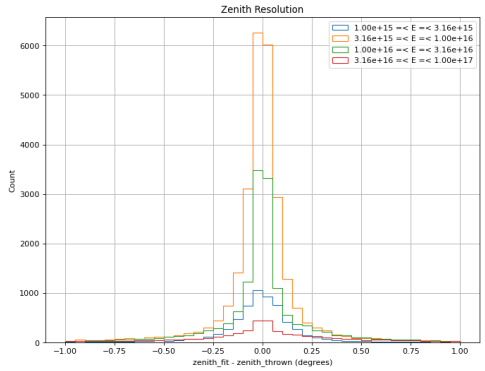

Figure 9: The zenith angle resolution. The resolution is shown for half-decade in energy bands which are not normalized and thus represent the thrown E^{-2} spectrum combined with trigger efficiency.

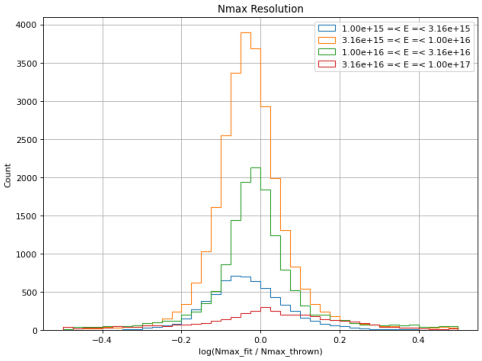

Figure 10: The resolution in measuring $N_{\max}$. The resolution is shown for half-decade in energy bands which are not normalized and thus represent the thrown E^{-2} spectrum combined with trigger efficiency.

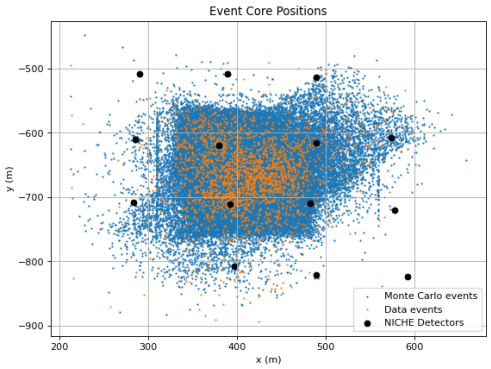

Figure 11: A comparison of the MC reconstructed core positions with the NICHE data reconstructed positions demonstration the acceptance area of the NICHE array. For much of the collected data, the two right central detectors were inactive leading to a leftward shift in accepted events given that one of the central detectors was required to have the largest signal.

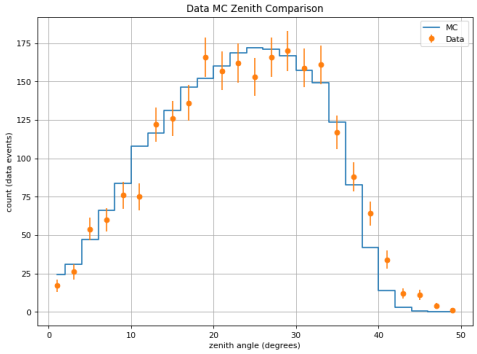

Figure 12: A comparison of the reconstructed zenith angle distribution for MC to that of data. A cut of $\theta < 32^\circ$ was made in the final analysis.

plots shown in the previous section.

The agreement in MC core positions and reconstructed data core positions is shown in Figure 11. As a contained event requirement, the largest signal in the six or more NICHE counters was required to be one of the four central detectors. Two of these central detectors were inactive for much of the run period consider in this analysis. The agreement in the reconstructed zenith angles of events in shown in Figure 12.

A final comparison of the reconstructed energy distribution is shown in Figure 13. The energy

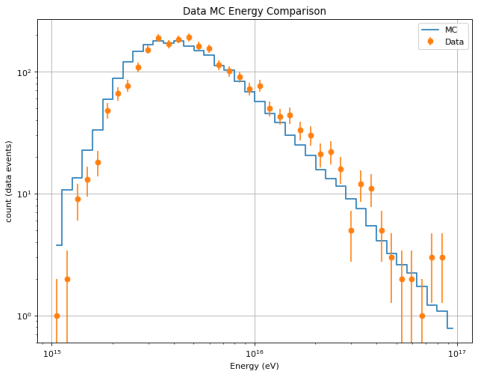

Figure 13: A comparison of the reconstructed energy distribution with the NICHE data energy distribution. The data energy distribution will go directly into the flux calculation.

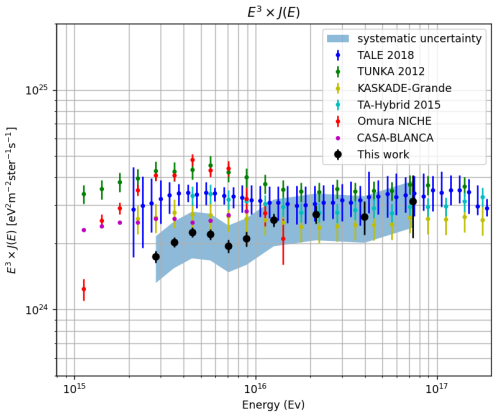

Figure 14: The spectrum of cosmic rays measured by the NICHE array. The flux measurements have been multiplied by E^3 to enhance feature identification. Several other spectrum measurements have been included for comparison.

reconstruction includes both $N_{\max}$ and $X_{\max}$ contributions. This figure also shows the data that will form the numerator of the flux calculation. There is a lower energy threshold evident for MC events than for the actual events. This is likely due to the lack of hadronic sub showers in the CHASM generation of NICHE events.

The final spectrum calculation using the NICHE data from perfect weather (no visible clouds from the TA MD operator) is shown in Figure 14. This spectrum include data from 165.1 hours live time for the detector. The difference between this work and that of [1] is notable. This is perhaps due to the much different calibration scheme as the energy scale seems to be quite different.

The Telescope Array experiment is supported by the Japan Society for the Promotion of Science(JSPS) through Grants-in-Aid for Priority Area 431, for Specially Promoted Research JP21000002, for Scientific Research (S) JP19104006, for Specially Promoted Research JP15H05693, for Scientific Research (S) JP19H05607, for Scientific Research (S) JP15H05741, for Science Research (A) JP18H03705, for Young Scientists (A) JPH26707011, and for Fostering Joint International Research (B) JP19KK0074, by the joint research program of the Institute for Cosmic Ray Research (ICRR), The University of Tokyo; by the Pioneering Program of RIKEN for the Evolution of Matter in the Universe (r-EMU); by the U.S. National Science Foundation awards PHY-1806797, PHY-2012934, PHY-2112904, PHY-2209583, PHY-2209584, and PHY-2310163, as well as AGS-1613260, AGS-1844306, and AGS-2112709; by the National Research Foundation of Korea (2017K1A4A3015188, 2020R1A2C1008230, and RS-2025-00556637) ; by the Ministry of Science and Higher Education of the Russian Federation under the contract 075-15-2024-541, IISN project No. 4.4501.18, by the Belgian Science Policy under IUAP VII/37 (ULB), by National Science Centre in Poland grant 2020/37/B/ST9/01821, by the European Union and Czech Ministry of Education, Youth and Sports through the FORTE project No. CZ.02.01.01/00/22_008/0004632, and by the Simons Foundation (00001470, NG). This work was partially supported by the grants of the joint research program of the Institute for Space-Earth Environmental Research, Nagoya University and Inter-University Research Program of the Institute for Cosmic Ray Research of University of Tokyo. The foundations of Dr. Ezekiel R. and Edna Wattis

Dumke, Willard L. Eccles, and George S. and Dolores Doré Eccles all helped with generous donations. The State of Utah supported the project through its Economic Development Board, and the University of Utah through the Office of the Vice President for Research. The experimental site became available through the cooperation of the Utah School and Institutional Trust Lands Administration (SITLA), U.S. Bureau of Land Management (BLM), and the U.S. Air Force. We appreciate the assistance of the State of Utah and Fillmore offices of the BLM in crafting the Plan of Development for the site. We thank Patrick A. Shea who assisted the collaboration with much valuable advice and provided support for the collaborationâ€™s efforts. The people and the officials of Millard County, Utah have been a source of steadfast and warm support for our work which we greatly appreciate. We are indebted to the Millard County Road Department for their efforts to maintain and clear the roads which get us to our sites. We gratefully acknowledge the contribution from the technical staffs of our home institutions. An allocation of computing resources from the Center for High Performance Computing at the University of Utah as well as the Academia Sinica Grid Computing Center (ASGC) is gratefully acknowledged.

References

[1] Y. Omura *et al.*, "Energy spectrum and the shower maxima of cosmic rays above the knee region measured with the NICHE detectors at the TA site," PoS(ICRC2021)329.

[2] I. Buckland and D.R. Bergman, "CHASM (CHerenkov Air Shower Model)," PoS(ICRC2023)325.

[3] D. Heck et al., Report FZKA 6019 (1998)

[4] E.E. Koresteleval *et al.*, Proc. 31st ICRC, Łódź, 492.